

Carbonyl substitution chemistry of some trimetallic transition metal cluster complexes with polyfunctional ligands

Lindsay T. Byrne^a, Nicole S. Hondow^a, George A. Koutsantonis^{a,*}, Brian W. Skelton^a,
A. Asgar Torabi^{a,1}, Allan H. White^a, S. Bruce Wild^b

^a Chemistry, M313, University of Western Australia, Crawley, WA 6009, Australia

^b Research School of Chemistry, Australian National University, Canberra, ACT 0200, Australia

Received 2 November 2007; received in revised form 23 January 2008; accepted 24 January 2008

Available online 2 February 2008

Abstract

The trimetallic clusters $[\text{Ru}_3(\text{CO})_{10}(\text{dppm})]$, $[\text{Ru}_3(\text{CO})_{12}]$ and $[\text{RuCo}_2(\text{CO})_{11}]$ react with a number of multifunctional secondary phosphine and tertiary arsine ligands to give products consequent on carbonyl substitution and, in the case of the secondary phosphines, PH activation. The reaction with the unresolved mixed P/S donor, 1-phenylphosphino-2-thio(ethane), $\text{HSCH}_2\text{CH}_2\text{PPh} (= \text{LH}_2)$, gave two products under various conditions which have been characterised by spectroscopic and crystallographic means. These two complexes $[\text{Ru}_3(\mu\text{-dppm})(\text{H})(\text{CO})_7(\text{LH})]$ and $[\text{Ru}_3(\mu\text{-dppm})(\text{H})(\text{CO})_8(\text{LH})\text{Ru}_3(\mu\text{-dppm})(\text{CO})_9]$, show the versatility of the ligand, with it chelating in the former and bridging two Ru_3 units in the latter. The stereogenic centres in the molecules gave rise to complicated spectroscopic data which are consistent with the presence of diastereoisomers. In the case of $[\text{Ru}_3(\text{CO})_{12}]$ the reaction with LH_2 gave a poor yield of a tetranuclear butterfly cluster, $[\text{Ru}_4(\text{CO})_{10}(\text{L})_2]$, in which two of the ligands bridge opposite hinge wingtip bonds of the cluster. A related ligand, $\text{HSCH}_2\text{CH}_2\text{AsMe}(\text{C}_6\text{H}_4\text{CH}_2\text{OMe})$, reacted with $[\text{RuCo}_2(\text{CO})_{11}]$ to give a low yield of the heterobimetallic Ru–Co adduct, $[\text{RuCo}(\text{CO})_6(\text{SCH}_2\text{CH}_2\text{AsMe}(\text{C}_6\text{H}_4\text{CH}_2\text{OMe}))]$, which appears to be the only one of its type so far structurally characterised.

The secondary phosphine, $\text{HPMe}(\text{C}_6\text{H}_4(\text{CH}_2\text{OMe}))$ and its oxide $\text{HP}(\text{O})\text{Me}(\text{C}_6\text{H}_4(\text{CH}_2\text{OMe}))$ also react with the cluster $[\text{Ru}_3(\text{CO})_{10}(\text{dppm})]$ to give carbonyl substitution products, $[\text{Ru}_3(\text{CO})_5(\text{dppm})(\mu_2\text{-PMe}(\text{C}_6\text{H}_4\text{CH}_2\text{OMe}))_4]$, and $[\text{Ru}_3\text{H}(\text{CO})_7(\text{dppm})(\mu_2, \eta^1\text{-P}(\text{=O})\text{Me}(\text{C}_6\text{H}_4\text{CH}_2\text{OMe}))]$. The former consists of an open Ru_3 triangle with four phosphide ligands bridging the metal–metal bonds; the latter has the O atom symmetrically bridging one Ru–Ru bond, the P atom being attached to a non-bridged Ru atom.

© 2008 Elsevier B.V. All rights reserved.

Keywords: Ruthenium; Cobalt; Carbonyl substitution; Cluster; Thiol; Secondary phosphine

1. Introduction

The oil industry is potentially reaching peak production and as such the time for the utilisation of more marginal crude oils is approaching, typically those containing large amounts of sulfurous compounds which require removal by hydrodesulfurization over catalysts promoted

by dihydrogen. This process creates large amounts of noxious sulfur containing effluent and this needs to be contained for both environmentally and industrially important reasons [1,2]. Thus, the efficient use of our remaining reserves is of utmost importance as some crude oils have significant sulfurous impurities that act to poison fluid cracking catalysts and it is timely that we understand the way in which sulfur interacts with small aggregates of metal atoms [3–5].

Organometallic complexes, containing two or more adjacent metals, have been presented as models for processes occurring at associated metal sites on the sur-

* Corresponding author. Tel./fax: +61 8 6488 3177/7247.

E-mail address: george.koutsantonis@uwa.edu.au (G.A. Koutsantonis).

¹ On leave from Zanjan University, Republic of Iran.

faces of heterogeneous catalysts [6–9], and, because such complexes may display novel reactivity, notably the expectation of enhanced selectivity, utilising the impact of mutually cooperative metals on substrate molecules. The role of the metal in dehydrosulfurization has been explored recently [3,10–12], showing that the interaction of chalcogenic ligands with transition metals is of major interest. The existence of several different metal atoms in an active catalyst provides many potential structural and chemical alternatives for multisite binding and catalysis of organic substrates or fragments on the metal particle [13].

The chemistry of $[\text{Ru}(\mu\text{-dppm})(\text{CO})_{10}]$ (dppm = 1,2-bis(diphenylphosphino)methane) [14] (**1**), is characterised by the straightforward addition of numerous groups without prior activation of the cluster [15]. The reactivity of **1** stems from the ability of the dppm ligand to prevent dissociation of metal centres from the cluster. The complex readily undergoes facile ligand transformation, eliminating benzene and orthometalating another phenyl substituent [16–19]. We have recently reported that the enhanced reactivity of $[\text{Ru}_3(\mu\text{-dppm})(\text{CO})_{10}]$ relative to the parent carbonyl $[\text{Ru}_3(\text{CO})_{12}]$ appeared to be a result of the inability of the cluster to effectively relieve steric congestion imposed by the presence of the bulky bidentate dppm ligand [15]. In extending this work we examine the reaction of polyfunctional ligands containing diverse functionality, particularly 1-phenylphosphino-2-thio(ethane), $\text{HSCH}_2\text{CH}_2\text{PPh}$ (= LH_2), with homometallic clusters $[\text{Ru}_3(\text{CO})_{12}]$ and $[\text{Ru}(\mu\text{-dppm})(\text{CO})_{10}]$, and heterometallic $[\text{RuCo}_2(\text{CO})_{11}]$. In this way the influences of various functionalities can be assessed for comparison with catalytic systems.

2. Experimental

2.1. Syntheses

The reactions were conducted under atmospheres of high purity argon using standard Schlenk techniques and tetrahydrofuran (THF) dried over potassium metal. $[\text{Ru}_3(\mu\text{-dppm})(\text{CO})_{10}]$ was prepared using the published procedure [20]. NMR spectra were measured on Bruker ARX 300 (^1H at 300.13 MHz, ^{13}C at 75.5 MHz and ^{31}P at 121.5 MHz) and Bruker ARX 500 (^1H at 500.13 MHz, ^{13}C at 125.8 MHz and ^{31}P at 202.4 MHz) spectrometers. Solution infrared spectra (CaF₂ cell) were acquired on a DigiLab Excalibur FTS-3000 spectrometer. Mass spectra were acquired on a VG Autospec spectrometer employing the Fast-Atom-Bombardment (FAB) technique. Elemental analyses were performed by Microanalytical Services, Research School of Chemistry, Australian National University. Preparative Thin Layer Chromatography was performed on glass plates (20 × 20 cm) coated with Silica Gel (Fluka, 60GF₂₅₄). The ligand LH_2 was prepared according to literature procedures [21] and references therein.

2.1.1. Preparation of $[\text{Ru}_3(\mu\text{-dppm})(\text{H})(\text{CO})_7(\text{SCH}_2\text{CH}_2\text{PPhH})]$ (**2**) and $[\text{Ru}_3(\mu\text{-dppm})(\text{H})(\text{CO})_8(\text{SCH}_2\text{CH}_2\text{PPhH})\text{Ru}_3(\mu\text{-dppm})(\text{CO})_9]$ (**3**)

To a solution of $[\text{Ru}_3(\mu\text{-dppm})(\text{CO})_{10}]$ (**1**) (500 mg, 0.70 mmol) in toluene (80 mL) was added LH_2 (80 μL , 0.70 mmol). The resulting solution was stirred and gently warmed (ca. 60 °C) for 2 h. The solvent was removed in vacuo and the residue chromatographed (TLC, 1/5 acetone–hexanes) and the three resulting bands collected. The first band ($R_f = 0.35$) was established (by IR) to be unreacted starting material **1** (172 mg, 34%).

The second band ($R_f = 0.28$) was crystallised from acetone to give red crystals of **2** (80 mg, 15%). X-ray quality crystals were grown from $\text{CH}_2\text{Cl}_2/\text{EtOH}$. Anal. Calc. for $\text{C}_{40}\text{H}_{33}\text{O}_7\text{P}_3\text{SRu}_3 \cdot \text{CH}_2\text{Cl}_2$: C, 43.23; H, 3.10. Found: C, 42.84; H, 3.74%. IR (CH_2Cl_2): $\nu(\text{CO})$ 2065w, 2052w, 2032m, 1988vs, 1979vs, 1961s cm^{-1} . ^1H NMR (acetone-*d*₆; 500 MHz) (nb. coupling constants for major isomer only) δ 7.9–7.1 (m, Ph), 6.28 (d, 1H, $^1J_{\text{PH}} = 355$ Hz, PH(major)), 6.11 (ddd, 1H, $^1J_{\text{PH}} = 351$, $J = 9.9$, 3.6 Hz, PH(minor)), 5.11 (ddd, 1H(major) + 1H(minor), $^2J_{\text{HH}} = 15.3$ (geminal), $^2J_{\text{PH}} = 11.3$, 9.6 Hz, PCH₂P), 4.40 (dt, 1H(major) + 1H(minor), $^2J_{\text{HH}} = 15.3$ (geminal), $^2J_{\text{PH}} = 10.8$, 10.8 Hz, PCH₂P), 2.50 (m, 2H, PCH₂, major), 2.41 (m, 2H, PCH₂, minor), 2.09 (m, 2H, SCH₂, major + minor), 1.70 (m, 1H, SCH₂, major), 1.22 (m, 1H, SCH₂, minor), –15.74 (dd, 1H, $J = 41$, 10.5 Hz, RuH, minor) –15.99 (ddt, 1H, $J = 41$, 11.6, 2 Hz, RuH, major) $^{31}\text{P}\{^1\text{H}\}$ NMR (acetone-*d*₆) δ 37.49 (dd, $^3J_{\text{PP}} = 30.2$, 8.2 PH, minor), 31.97 (dd, $^3J_{\text{PP}} = 28.2$, 8.2 PH, major), 21.44 (m, PCH₂, minor), 21.86 (m, PCH₂, major), 14.28 (dd, obscured $^2J_{\text{PP}} = \text{ca. } 57$, $^3J_{\text{PP}} = 29.7$ Hz, PCH₂, minor), 14.02 (dd, obscured $^2J_{\text{PP}} = 51.8$, $^3J_{\text{PP}} = 27.8$ Hz, PCH₂, minor). FABMS (NOBA) m/z 1052, $[\text{M}^+]$; 1024–858, $[\text{M}-n\text{CO}]^+ n = 1-7$.

The third band ($R_f = 0.18$) was crystallised from acetone to give red crystals of **3** (158 mg, 15%). Crystals for analysis were grown from $\text{CH}_2\text{Cl}_2/\text{EtOH}$ and from acetone/hexane for X-ray structural determination. Anal. Calc. for $\text{C}_{75}\text{H}_{55}\text{O}_{17}\text{P}_4\text{SRu}_6 \cdot \text{CH}_2\text{Cl}_2$: C, 43.33; H, 2.73. Found: C, 43.31; H, 2.98%. IR (CH_2Cl_2): $\nu(\text{CO})$ 2065m, 2053w, 2020w, 1998vs, 1976vs, 1940m cm^{-1} . ^1H NMR (acetone-*d*₆) δ 7.7–7.1 (m, Ph), 5.73 (m, $^1J_{\text{PH}} = 400$ Hz, $^3J_{\text{HH}}$ is unresolved, PH), 5.05, 4.55 (m, 2H, $\mu\text{-dppm}$, unit B), 4.73 (br d, 2H, $\mu\text{-dppm}$, unit A), 2.35 (m, 2H, PCH₂), 1.87 (m, 2H, SCH₂), –14.95 (dd, 1H, $^2J_{\text{PH}} = 33$, $^3J_{\text{PH}} = 3.4$ Hz, RuH), –14.98 (dd, 1H, $^2J_{\text{PH}} = 33$, $^3J_{\text{PH}} = 3.4$ Hz, RuH). ^{31}P NMR (acetone-*d*₆) δ 20.52 (d, $^2J_{\text{PP}} = 44$ Hz, dppm, Unit A), 20.33 (d, $^2J_{\text{PP}} = 44$ Hz, dppm, Unit A), 16.24 (d, $^2J_{\text{PP}} = 44$ Hz, dppm, Unit A), 16.1 (m, dppm, Unit B), 15.82 (d, $^2J_{\text{PP}} = 44$ Hz, dppm, Unit A), –3.10 (t, J ca. 11 Hz, PH), –4.09 (t, ca. 11 Hz, PH). FABMS (NOBA) m/z 2020, $[\text{M}^+]$.

2.1.2. Preparation of $[\text{Ru}_4(\text{CO})_{10}(\text{SCH}_2\text{CH}_2\text{PPh})_2]$ (**4**)

To a solution of $[\text{Ru}_3(\text{CO})_{12}]$ (100 mg, 0.16 mmol) in THF (80 mL) was added LH_2 (22 μL , 0.56 mmol) and five

drops of a sodium benzophenone ketyl solution. The resulting solution was stirred for 13 h and the solvent was removed in vacuo and the residue chromatographed (TLC, 30:70; acetone–hexanes). The only tractable and major red band (R_f 0.76) was collected and crystallised from CH_2Cl_2 /hexanes giving red needles of **4** (24 mg, 22%). Anal. Calc. for $\text{C}_{26}\text{H}_{18}\text{O}_{10}\text{P}_2\text{Ru}_4\text{S}_2$: C, 30.59; H, 1.78. Found: C, 30.99; H, 1.42%. IR (CH_2Cl_2): $\nu(\text{CO})$ 2088w, 2049s, 2011s, 1993sh, 1978sh. FABMS (NOBA) m/z 1023, $[\text{M}^+]$.

2.1.3. Preparation of $[\text{RuCo}(\text{CO})_6(\text{SCH}_2\text{CH}_2\text{AsMe}(\text{C}_6\text{H}_4\text{CH}_2\text{OMe}))]$ (**5**)

A solution of $\text{HSCH}_2\text{CH}_2\text{AsMe}(\text{C}_6\text{H}_4\text{CH}_2\text{OMe})$ (73 mg, 0.27 mmol) in hexane (10 mL) was added to a solution of $[\text{RuCo}_2(\text{CO})_{11}]$ (151 mg, 0.29 mmol) in hexane (20 mL) dropwise by cannula, dissipating the initial red colour. After standing at room temperature overnight the brown-yellow suspension was filtered by cannula, concentrated in vacuo and stored at low temperature (-22°C) to afford brown crystals of **5** (52 mg, 30%). Anal. Calc. for $\text{C}_{17}\text{H}_{16}\text{AsCoO}_7\text{RuS}$: C, 34.07; H, 2.69. Found: C, 33.86; H, 2.47%. M.p. $>150^\circ\text{C}$ (dec). ^1H NMR δ (d_6 -benzene) 1.38 (s, 3H, AsCH_3); 1.62, 1.85, 2.05, 2.50 (m, 4H, $\text{AsCH}_2\text{CH}_2\text{S}$); 3.04 (s, 3H, OCH_3); 4.08 (AB pattern, 2H, $J_{\text{AB}} = 12$ Hz, CH_2OCH_3); 6.59, 6.81, 6.95, 7.03 (m, 4H, C_6H_4) ^{13}C NMR δ (d_6 -benzene) 13.2 (AsCH_3), 29.3 ($\text{AsCH}_2\text{CH}_2\text{S}$), 32.7 ($\text{AsCH}_2\text{CH}_2\text{S}$), 58.0 (OCH_3), 130.9, 130.3, 136.3, 139.9 (Ph), 189.0, 192.7, 200.2, 208.8 (M-CO). FAB-MS (NOBA) 600, $[\text{M}^+]$, 100; 572–488, $[\text{M}^+ - n\text{CO}]$.

2.1.4. Preparation of $[\text{Ru}_3(\text{CO})_5(\mu\text{-dppm})(\text{PMe}(\text{C}_6\text{H}_4\text{CH}_2\text{OMe}))_4]$ (**6**) and $[\text{Ru}_3\text{H}(\text{CO})_7(\mu\text{-dppm})(\text{P}(=\text{O})\text{Me}(\text{C}_6\text{H}_4\text{CH}_2\text{OMe}))]$ (**7**)

A solution of $[\text{Ru}_3(\mu\text{-dppm})(\text{CO})_{10}]$ (**1**) (100 mg, 0.10 mmol) in THF was treated with $\text{HPMe}(\text{C}_6\text{H}_4\text{CH}_2\text{OMe})$ (16 μl , 0.10 mmol) and heated to reflux for 7 h. The resulting dark red solution was evaporated to dryness and attempted crystallisation of the residue from CH_2Cl_2 /hexanes gave a small amount of **6** overnight (19 mg, 13%). Anal. Calc. for $\text{C}_{66}\text{H}_{70}\text{O}_9\text{P}_6\text{Ru}_3$: C, 52.98; H, 4.72. Found: C, 51.14; H, 4.65%. IR (CH_2Cl_2): $\nu(\text{CO})$ 2008w, 1977s, 1944w, 1919s, 1909sh. FABMS (NOBA) m/z 1499, $[\text{M}^+]$.

The supernatant was subjected to preparative TLC giving four bands (R_f 0.66, red; R_f 0.59, yellow; R_f 0.51, red; R_f 0.44, yellow) and significant decomposition. None of these bands gave appreciable material on work-up.

In a another reaction analogous to the one above, a solution of $[\text{Ru}_3(\mu\text{-dppm})(\text{CO})_{10}]$ (**1**) (200 mg, 0.21 mmol) in THF was treated with an excess of $\text{HPMe}(\text{C}_6\text{H}_4\text{CH}_2\text{OMe})$ {presumably contaminated with $\text{HP}(=\text{O})\text{Me}(\text{C}_6\text{H}_4\text{CH}_2\text{OMe})$ } (128 μl , 0.83 mmol). Crystallisation of the dark residue obtained from the reaction gave a small amount of **7** (49 mg, 22%). Anal. Calc. for $\text{C}_{41}\text{H}_{35}\text{O}_9\text{P}_3\text{Ru}_3$: C, 46.12; H, 3.30. Found: C, 45.63; H, 2.67%. IR (CH_2Cl_2):

$\nu(\text{CO})$ 2035s, 2021s, 1987w, 1968s, 1937sh. FABMS (NOBA) m/z 1068, $[\text{M}^+]$.

2.2. Structure determinations

For **2**, **3**, **6**, **7**, full spheres of CCD area-detector diffractometer data were measured (Bruker AXS instrument, ω -scans; monochromatic Mo $\text{K}\alpha$ radiation, $\lambda = 0.71073 \text{ \AA}$; T ca. 153 K); for **4**, synchrotron radiation ($\lambda = 0.5594 \text{ \AA}$) was employed (T ca. 110 K). $N_{(\text{total})}$ reflections were obtained, these merging to N unique (R_{int} cited) after 'empirical'/multiscan absorption correction (proprietary software), N_o with $F > 4\sigma(F)$ considered 'observed'. Full matrix least squares refinements on all data, refined anisotropic displacement parameter forms for the non-hydrogen atoms, $(x, y, z, U_{\text{iso}})_\text{H}$ being included following a riding model; reflection weights were $(\sigma^2(F) + (aP)^2 + bP)^{-1}$ ($P = F_o^2 + 2F_c^2/3$). For **5**, a unique, single-counter diffractometer data set was measured; T was 295 K. Neutral atom complex scattering factors were employed within the context of the SHELX 97 program [22]. Pertinent results are given below and in the tables and figures, the latter showing 50% probability amplitude displacement envelopes for the non-hydrogen atoms. Individual variations in procedure are noted as 'variata'.

2.2.1. Variata

3: Phenyl ring 52n was modelled as disordered over two sets of sites, occupancies refining to 0.66(1) and complement (isotropic displacement parameters for the minor C_6 component). The core hydride atoms were located by refinement in $(x, y, z, U_{\text{iso}})_\text{H}$.

4: A number of significant difference map residues ($<3 \text{ e \AA}^{-3}$) were observed in the vicinity of the ruthenium core, not susceptible of sensible modelling and suggestive of core disorder or cocrystallized minor impurity.

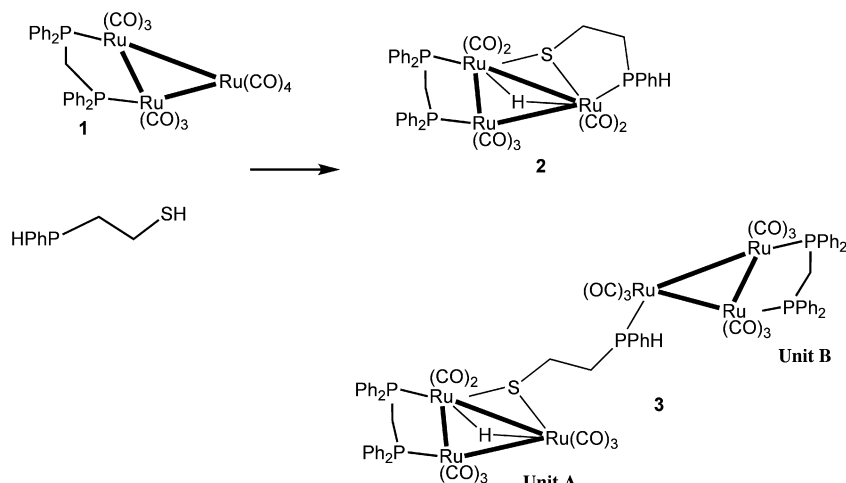
5: Material was badly twinned; overlapping reflections were refined as a separately scaled group.

6: Solvent residues were modelled in terms of disordered CH_2Cl_2 (site occupancies for one molecule disordered over two sites, set at 0.5 with the other, also disordered over three sites, set at 0.33) with idealised geometries. Methoxyl groups 412, 512, 612 were modelled as disordered over pairs of sites, occupancies set at 0.5 after trial refinement, ring 51n being similarly disordered.

7: Solvent CH_2Cl_2 was modelled as disordered about a crystallographic inversion centre.

3. Results and discussion

The substituted ruthenium carbonyl cluster **1** is reactive and well known to undergo substitution reactions with phosphine ligands [15]. In addition, simple thiols, such as PhSH , are known to add across a Ru–Ru bond [23]. In the former case the P donor substitutes an equatorial CO, whereas the latter gives the thiolato hydrido cluster in which the bridging H and SPh ligands span the same



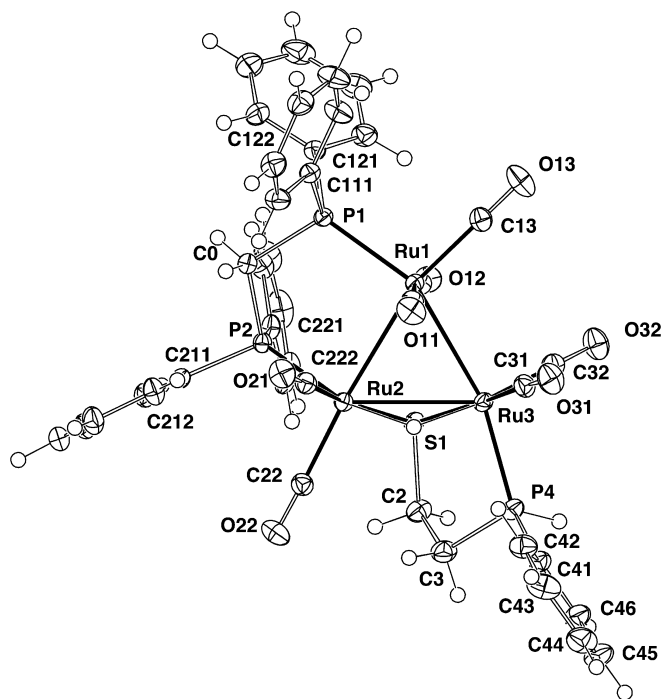
Scheme 1.

Ru–Ru bond. The 2-(phenylphosphine)ethanethiol ligand, $\text{HPhPCH}_2\text{CH}_2\text{SH}$ ($= \text{LH}_2$), has additional functionality in the form of a secondary phosphine and it was of interest to observe the mode of reaction with **1** in light of this surfeit of functionality. When the reaction occurred at the temperature of refluxing toluene a large number of intractable products were formed. Under ambient conditions the reaction was very slow and in some cases considerable decomposition was also observed. However, the reaction of LH_2 with **1** in toluene at 60°C presented a mixture of three complexes on work up by TLC, Scheme 1. There was an appreciable amount of residual starting material returned and two new products, which were characterised by microanalysis, standard spectroscopic techniques, and by single-crystal

X-ray diffraction studies as **2** and **3**. When the reaction was carried out with an excess of ligand present, a number of products were isolated but none of these corresponded to **2** or **3** and they are yet to be identified. Activating the cluster to substitution utilising sodium benzophenone ketyl radical did not improve the yields of **2** or **3** nor did performing the reaction overnight at 60°C .

The IR spectra of the complexes **2** and **3** contained bands that are consistent with terminal CO ligands and their FAB mass spectra contained molecular ions which lost consecutive CO ligands in the case of complex **2**.

The two complexes gave complicated NMR spectra consistent with the presence of the stereogenic centres in the molecules. The presence of metal bound hydrides was inferred from the upfield resonances found in proton NMR spectra.

Fig. 1. Molecular projection of the structure of **2**.Table 1
Selected geometries (**2**)

Atoms	Parameter	Atoms	Parameter
<i>Distances (Å)</i>			
Ru(1)–Ru(2)	2.8446(3)	Ru(1)–P(1)	2.3176(6)
Ru(1)–Ru(3)	2.8191(3)	Ru(2)–P(2)	2.3167(6)
Ru(2)–Ru(3)	2.8712(3)	Ru(2)–C(21)	1.879(2)
Ru(1)–C(11)	1.924(2)	Ru(2)–C(22)	1.902(3)
Ru(1)–C(12)	1.940(2)	Ru(2)–S(1)	2.4040(6)
Ru(1)–C(13)	1.899(3)	Ru(3)–S(1)	2.3875(6)
Ru(2)–H	1.65(4)	Ru(3)–C(31)	1.889(2)
Ru(3)–H	1.77(4)	Ru(3)–C(32)	1.874(3)
		Ru(3)–P(4)	2.3064(7)
<i>Angles (°)</i>			
Ru(2)–Ru(1)–Ru(3)	60.921(8)	P(2)–Ru(2)–Ru(1)	85.35(2)
Ru(1)–Ru(2)–Ru(3)	59.101(7)	P(2)–Ru(2)–Ru(3)	136.11(2)
Ru(1)–Ru(3)–Ru(2)	59.978(6)	P(2)–Ru(2)–S(1)	100.11(2)
P(1)–Ru(1)–Ru(2)	95.00(2)	Ru(1)–Ru(2)–S(1)	80.90(2)
P(1)–Ru(1)–Ru(3)	155.89(2)	Ru(3)–Ru(2)–S(1)	52.92(2)
Ru(1)–Ru(3)–P(4)	163.93(2)	Ru(2)–S(1)–Ru(3)	73.63(2)
Ru(1)–Ru(3)–S(1)	81.71(2)	Ru(2)–S(1)–C(2)	109.99(9)
Ru(2)–Ru(3)–P(4)	105.34(2)	Ru(3)–S(1)–C(2)	106.27(8)
Ru(2)–Ru(3)–S(1)	53.45(2)	S(1)–Ru(3)–P(4)	83.92(2)
		Ru(3)–P(4)–C(3)	107.28(8)

The NMR spectra measured for **3** suggested the presence of isomeric, presumably diastereomeric, species in equal ratio. The $^{31}\text{P}\{^1\text{H}\}$ NMR spectrum measured for complex **3** clearly illustrates this point as it contains two essentially identical, in some parts overlapping, sets of resonances. In recent work we have unequivocally assigned the $^{31}\text{P}\{^1\text{H}\}$ NMR spectra of $[\text{Ru}_3(\text{CO})_9(\text{dppm})(\text{PR}_3)]$ [15] complexes which are analogous to segment **B** of complex **3** while segment **A** observes close similarity to the well-known sulfido clusters $[\text{Ru}_3(\mu\text{-H})(\mu\text{-SR})(\text{CO})_8(\text{dppm})]$ [23]. Thus, the complex multiplet centered at ca. 16.0 ppm in the $^{31}\text{P}\{^1\text{H}\}$ NMR spectrum of **3** is assigned to the $\mu\text{-dppm}$ of unit **B**. Signals attributable to the analogous bidentate ligand of unit **A** are partly obscured by this resonance but the doublets at δ 20.52, 20.33, 16.24 and 15.82 ppm, with characteristic $^2J_{\text{PP}} = 44$ Hz [23], were assigned to the inequivalent P atoms of the $\mu\text{-dppm}$ ligand

in the diastereoisomers. The other two overlapping doublets of doublets observed at δ -3.10 and -4.09 ppm ($^3J_{\text{PP}}$ ca. 10 Hz, ca. 11 Hz), significantly downfield of the free ligand [21], are assigned to the diastereomeric PH moieties of the phenylphosphinoethanethiol ligand, on the basis of the proton-coupled ^{31}P NMR spectrum which showed a $^1J_{\text{PH}} = 348$ Hz for each of these resonances. These signals are coupled to the P atoms of the $\mu\text{-dppm}$ ligand of unit **B** with a coupling constant of ca. 11 Hz.

The presence of a metal hydride was inferred by the presence of two doublets of doublets observed at ca. -15 ppm ($^2J_{\text{PH}} = 33.0$; $^3J_{\text{PH}} = 3.4$ Hz) in the ^1H NMR spectrum of **3** resulting from coupling to the two inequivalent phosphorus atoms of unit **A**, each set of doublet of doublets suggesting an equivalent mixture of diastereoisomers. The primary phosphine PH resonance is assigned to the complex multiplet centred on δ 5.73

Table 2
Selected geometries (**3**) (molecules 1 and 2)

Atoms	Parameter	Atoms	Parameter
Distances (Å)			
<i>Segment A (for counterpart Ru in molecule 2, read 7–9 for 1–3)</i>			
Ru(1)–Ru(2)	2.8344(6), 2.8356(7)	Ru(2)–P(2)	2.316(1), 2.314(2)
Ru(1)–Ru(3)	2.8143(6), 2.8095(7)	Ru(2)–S(1)	2.393(1), 2.387(1)
Ru(2)–Ru(3)	2.8594(7), 2.8654(7)	Ru(2)–H	1.71(7), 1.86(6)
Ru(1)–P(1)	2.322(1), 2.324(2)	Ru(2)–C(21)	1.876(5), 1.874(6)
Ru(1)–C(11)	1.921(6), 1.918(6)	Ru(2)–C(22)	1.901(6), 1.904(6)
Ru(1)–C(12)	1.932(5), 1.949(6)	Ru(3)–S(1)	2.393(1), 2.389(2)
Ru(1)–C(13)	1.899(6), 1.895(6)	Ru(3)–C(31)	1.904(6), 1.894(7)
Ru(3)–H	1.68(7), 1.70(8)	Ru(3)–C(32)	1.903(6), 1.888(7)
		Ru(3)–C(33)	1.924(6), 1.914(7)
<i>Segment B (for counterpart Ru in molecule 2, read 10–12 for 4–6)</i>			
Ru(4)–Ru(5)	2.8353(6), 2.8442(6)	Ru(5)–P(5)	2.325(2), 2.330(1)
Ru(4)–Ru(6)	2.8460(7), 2.8434(7)	Ru(5)–C(51)	1.931(5), 1.922(5)
Ru(5)–Ru(6)	2.8490(6), 2.8449(6)	Ru(5)–C(52)	1.919(6), 1.933(5)
Ru(4)–P(4)	2.326(1), 2.318(1)	Ru(5)–C(53)	1.889(5), 1.887(6)
Ru(4)–C(41)	1.932(5), 1.935(6)	Ru(6)–P(6)	2.308(1), 2.295(1)
Ru(4)–C(42)	1.927(5), 1.931(5)	Ru(6)–C(61)	1.932(5), 1.922(6)
Ru(4)–C(43)	1.888(5), 1.885(5)	Ru(6)–C(62)	1.924(5), 1.936(6)
		Ru(6)–C(63)	1.890(5), 1.892(6)
Angles (°)			
<i>Segment A (n = 1,3)</i>			
Ru(2)–Ru(1)–Ru(3)	60.82(2), 61.06(2)	Ru(1)–Ru(2)–P(2)	86.39(3), 86.47(4)
Ru(1)–Ru(2)–Ru(3)	59.24(1), 59.05(2)	Ru(3)–Ru(2)–P(2)	135.65(4), 135.99(4)
Ru(2)–Ru(3)–Ru(1)	59.94(2), 59.95(2)	S(1)–Ru(2)–Ru(1)	82.03(3), 80.99(4)
P(1)–Ru(1)–Ru(2)	93.81(3), 93.76(4)	S(1)–Ru(2)–P(2)	98.25(5), 98.42(5)
P(1)–Ru(1)–Ru(3)	154.61(4), 154.75(4)	S(1)–Ru(2)–Ru(3)	53.30(3), 53.16(4)
Ru(2)–S(1)–Ru(3)	73.38(4), 73.74(4)	S(1)–Ru(3)–Ru(1)	82.48(3), 81.50(4)
Ru(2)–S(1)–C(2)	107.6(2), 107.7(2)	S(1)–Ru(3)–Ru(2)	53.33(3), 53.10(3)
Ru(3)–S(1)–C(2)	108.4(2), 107.8(2)		
<i>Segment B</i>			
Ru(5)–Ru(4)–Ru(6)	60.19(1), 60.02(2)	Ru(4)–Ru(5)–Ru(6)	60.09(2), 59.97(2)
Ru(5)–Ru(4)–P(4)	89.47(4), 93.73(4)	Ru(4)–Ru(5)–P(5)	94.60(4), 89.15(4)
Ru(6)–Ru(4)–P(4)	148.06(4), 150.49(4)	Ru(6)–Ru(5)–P(5)	152.86(4), 147.78(4)
Ru(4)–Ru(6)–Ru(5)	59.72(2), 60.00(2)	P(6)–Ru(6)–Ru(5)	97.65(4), 101.16(4)
P(6)–Ru(6)–Ru(4)	153.46(4), 156.90(6)	P(4)–C(20)–P(5)	115.9(3), 114.6(4)
Ru(6)–P(6)–C(3)	117.6(2), 115.4(2)	C(3)–P(6)–C(611)	104.5(2), 105.0(3)
Ru(6)–P(6)–C(611)	117.5(6), 115.8(2)		

P(n1, n2) deviant by $-0.040(3)$, $1.136(2)$; $-0.043(3)$, $1.106(2)$ Å (molecules 1 and 2); the skewing of P(n2)/CO(n21) relative to the Ru₃ plane is much less than that of CO(n31/n32), presumably in consequence of the chelate constraint.

The thermally activated reaction of [Ru₃(CO)₁₂] with LH₂, resulted in total decomposition. However, the analogous radical initiated reaction gave only one tractable product after chromatography, which was identified on the basis of a single crystal X-ray study as [Ru₄(CO)₁₀(μ₂:μ₂-

SCH₂CH₂PPh)₂], **4**, (Chart 1). In this case the phenylphosphino component of LH₂ has been deprotonated and is manifested as a bridging phosphido ligand and the thiol also adopts a bridging mode; in both cases the hydrogen attached to the heteroatom was lost. As a consequence of insolubility we were unable to obtain any spectroscopic data on the complex. In fact, the size of the crystals obtained after multiple attempts at crystallisation necessitated the collection of data for the single crystal study at a synchrotron.

Compound **4** crystallizes unsolvated with two independent neutral molecules, devoid of crystallographic symmetry, comprising the asymmetric unit of the structure, confirming the stoichiometry, connectivity and stereochemistry as given above (see also Fig. 3, Table 3). Despite the above comments, the molecular symmetry is close to 2, although across equivalent parameters between the (four) possibilities, individual excursions from their mean may be substantial. The core of each molecule is an Ru₄ 'butterfly', the fold angles across Ru(n1)–Ru(n2) being $139.38(4)^\circ$ and $138.28(4)^\circ$. Within the pair of Ru₃ planes so defined, the distances are dissimilar within each plane, the bond not fusing the two planes or bridged by the P,S-ligand the longest, and the fusing bond the shortest. The intermediate bond is straddled by the chelate, L, both S- and P-donors bridging the two ruthenium atoms μ₂ and lying to either side of the associated Ru₃ plane. The SCCP string is essentially planar, with the two associated Ru atoms

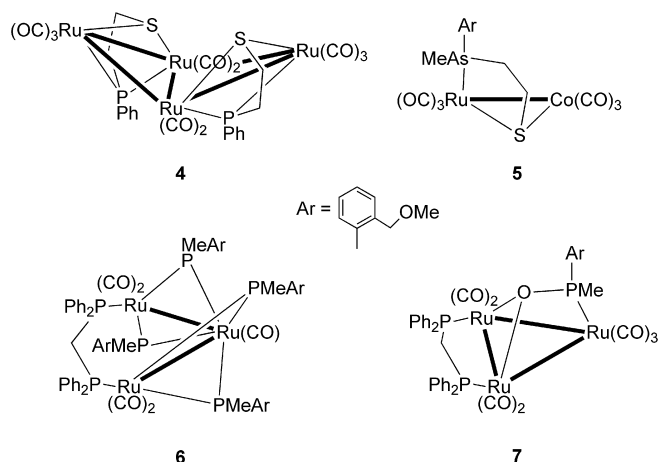
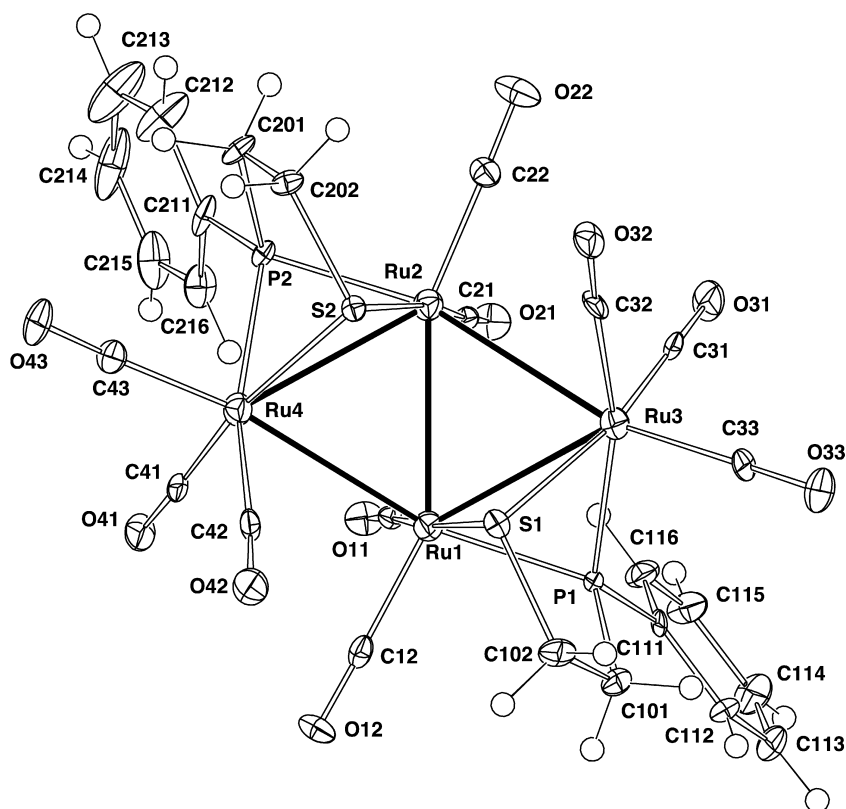


Chart 1.

Fig. 3. Molecular projection of one of the formula units in the structure of **4**.

lying to either side. Interestingly, the phenyl groups pendant from the phosphorus atoms are quasi-coplanar with the 'C₂SP' planes, despite close approaches between one of the ortho hydrogen atoms H(nm12) and the adjacent methylene hydrogen, in all cases ca. 2.3–2.4 Å (est.), and despite the C–P–C angle being less than the tetrahedral value; Ru–P–C (phenyl) in all cases are very large, 123.8(2)–127.9(2)°. The other ortho hydrogen is directed toward the alternate carbonyl oxygen of the pair of carbonyls which lie beneath the fold, with an appreciable torsion;

the closest such contact (H(2116)···O(221)) is 2.65 Å (est.). Among the carbonyl groups, there is little difference between the Ru–C distances for the pairs on the 'fold' Ru atoms; at the peripheral atoms Ru–C(CO) are longer, with the distance to the carbonyl lying adjacent to the sulfur the longest of all. There are a number of examples of this type of cluster in the literature, two salient examples being [Ru₄(μ₄-k⁴-dmpu)(CO)₁₀], (H₂dmpu = *N,N'*-bis(6-methylpyridin-2-yl)urea) [24] and [Ru₄(CO)₁₃(μ-PPH₂)₂] and [Ru₄(CO)₁₀(μ-PPH₂)₄] [25].

Table 3
Selected geometries (4) (molecules 1 and 2)

Atoms	Parameter	Atoms	Parameter	< >
<i>Distances (Å) (in molecule 2 read 1–4 as counterparts 5–8)</i>				
Ru(1)–Ru(2)	2.877(1), 2.856(1)			2.867(13)
Ru(1)–Ru(3)	2.914(1), 2.973(1)	Ru(2)–Ru(4)	2.966(1), 2.931(1)	2.95(3)
Ru(1)–Ru(4)	3.042(1), 3.007(1)	Ru(2)–Ru(3)	3.012(1), 3.026(1)	3.02(2)
Ru(1)–S(1)	2.396(2), 2.417(2)	Ru(2)–S(2)	2.412(1), 2.411(2)	2.409(9)
Ru(1)–P(1)	2.275(2), 2.255(2)	Ru(2)–P(2)	2.256(2), 2.270(2)	2.263(9)
Ru(3)–S(1)	2.408(2), 2.399(2)	Ru(4)–S(2)	2.387(2), 2.407(2)	2.399(11)
Ru(3)–P(1)	2.349(2), 2.332(2)	Ru(4)–P(2)	2.353(2), 2.344(2)	2.344(9)
Ru(1)–C(11)	1.880(6), 1.875(6)	Ru(2)–C(21)	1.885(6), 1.880(6)	1.879(8)
Ru(1)–C(12)	1.863(6), 1.880(6)	Ru(2)–C(22)	1.880(6), 1.880(6)	1.883(11)
Ru(3)–C(33)	1.921(6), 1.909(6)	Ru(4)–C(43)	1.907(6), 1.909(6)	1.912(10)
Ru(3)–C(31)	1.917(6), 1.927(6)	Ru(4)–C(41)	1.908(7), 1.918(6)	1.918(15)
Ru(3)–C(32)	1.948(6), 1.970(6)	Ru(4)–C(42)	1.957(6), 1.959(6)	1.964(14)
<i>Angles (°)</i>				
Ru(2)–Ru(1)–Ru(3)	62.67(2), 62.51(2)	Ru(1)–Ru(2)–Ru(4)	62.74(2), 62.60(2)	62.64(10)
Ru(2)–Ru(1)–Ru(4)	60.06(2), 59.92(2)	Ru(1)–Ru(2)–Ru(3)	59.27(2), 60.64(2)	60.0(6)
Ru(2)–Ru(1)–S(1)	89.34(4), 89.49(4)	Ru(1)–Ru(2)–S(2)	88.93(4), 89.03(5)	89.2(3)
Ru(2)–Ru(1)–P(1)	108.33(4), 105.74(5)	Ru(1)–Ru(2)–P(2)	107.19(5), 107.92(5)	107.3(12)
Ru(3)–Ru(1)–Ru(4)	110.81(3), 109.96(3)	Ru(4)–Ru(2)–Ru(3)	110.24(2), 110.61(3)	110.4(4)
Ru(3)–Ru(1)–S(1)	52.84(4), 51.68(4)	Ru(4)–Ru(2)–S(2)	51.44(4), 52.46(4)	52.1(7)
Ru(3)–Ru(1)–P(1)	52.06(4), 50.78(4)	Ru(4)–Ru(2)–P(2)	51.41(5), 51.68(4)	51.5(6)
Ru(4)–Ru(1)–S(1)	91.20(4), 91.77(4)	Ru(3)–Ru(2)–S(2)	92.15(4), 90.34(4)	91.4(8)
Ru(4)–Ru(1)–P(1)	162.21(5), 160.59(5)	Ru(3)–Ru(2)–P(2)	161.43(5), 161.38(5)	161.4(7)
S(1)–Ru(1)–P(1)	74.50(5), 74.18(5)	S(1)–Ru(2)–P(2)	74.01(5), 74.13(5)	74.2(2)
Ru(1)–Ru(3)–Ru(2)	58.06(2), 56.85(2)	Ru(2)–Ru(4)–Ru(1)	57.20(2), 57.48(2)	57.4(5)
Ru(1)–Ru(3)–S(1)	52.47(4), 52.14(4)	Ru(2)–Ru(4)–S(2)	52.24(3), 52.61(4)	52.4(2)
Ru(1)–Ru(3)–P(1)	49.82(4), 48.48(4)	Ru(2)–Ru(4)–P(2)	48.52(4), 49.45(4)	49.1(7)
Ru(2)–Ru(3)–S(1)	86.00(4), 85.90(4)	Ru(1)–Ru(4)–S(2)	85.60(4), 85.66(4)	85.8(2)
Ru(2)–Ru(3)–P(1)	102.17(4), 98.70(4)	Ru(1)–Ru(4)–P(2)	99.67(4), 101.30(4)	100.5(15)
S(1)–Ru(3)–P(1)	72.99(5), 73.15(5)	S(2)–Ru(4)–P(2)	72.79(5), 72.93(5)	72.96(14)
Ru(1)–S(1)–Ru(3)	74.70(4), 76.26(4)	Ru(2)–S(2)–Ru(4)	76.32(5), 74.94(4)	75.6(9)
Ru(1)–S(1)–C(102)	101.5(2), 101.7(2)	Ru(2)–S(2)–C(202)	102.2(2), 101.0(2)	101.8(4)
Ru(3)–S(1)–C(102)	104.7(2), 101.9(2)	Ru(4)–S(2)–C(202)	102.5(2), 104.7(3)	104(2)
Ru(1)–P(1)–Ru(3)	78.12(5), 80.74(5)	Ru(2)–P(2)–Ru(4)	80.07(6), 78.87(5)	79.5(12)
Ru(1)–P(1)–C(101)	108.5(2), 108.3(2)	Ru(2)–P(2)–C(201)	108.2(2), 108.4(2)	108.2(4)
Ru(3)–P(1)–C(101)	106.5(2), 106.2(2)	Ru(4)–P(2)–C(201)	106.5(3), 106.6(2)	106.6(3)
C(111)–P(1)–C(101)	105.7(3), 107.7(3)	C(211)–P(2)–C(201)	106.7(3), 106.3(3)	106.5(10)
Ru(1)–P(1)–C(111)	127.9(2), 126.9(2)	Ru(2)–P(2)–C(211)	125.6(2), 127.5(2)	127.1(10)
Ru(3)–P(1)–C(111)	126.8(2), 123.8(2)	Ru(4)–P(2)–C(111)	126.7(2), 126.0(2)	125.9(15)
<i>Torsion angles (°) (carbon atoms denoted by number only)</i>				
Ru(1)–S(1)–102–101	42.7(5), 38.0(5)	Ru(2)–S(2)–202–201	36.7(5), 43.0(4)	
S(1)–102–101–P(21)	–5.9(5), –0.3(6)	S(2)–202–201–P(2)	1.3(6), –6.0(5)	
Ru(1)–P(21)–101–102	–36.9(4), –42.3(5)	Ru(2)–P(2)–201–202	–43.5(5), –37.7(5)	
101–P(1)–111–112	–8.2(6), –6.9(6)	201–P(2)–211–212	8.4(7), –3.4(5)	
11–Ru(1)–Ru(2)–21	–30.7(2), –29.5(2)	S(1)–Ru(1)–Ru(2)–S(2)	–45.52(5), –45.01(5)	
<i>Out-of-plane deviations (δ, Å)</i>				
δS(1)(Ru ₃)	–1.770(2), 1.736(2)	δS(2)(Ru ₃)	–1.743(2), 1.773(2)	
δP(1)(Ru ₃)	0.940(2), –1.001(3)	δP(2)(Ru ₃)	0.967(2), –0.934(2)	

The heterobimetallic cluster $[\text{RuCo}_2(\text{CO})_{11}]$ has a well developed chemistry [26–29]. The existence of several different metal atoms in a metal cluster provides many potential structural and chemical opportunities for multisite binding and catalysis of organic substrates or fragments on a metal particle. The reaction between $[\text{RuCo}_2(\text{CO})_{11}]$ and $\text{HSCH}_2\text{CH}_2\text{AsMe}(\text{C}_6\text{H}_4\text{CH}_2\text{OMe})$ gave an extremely air-sensitive solution from which a low yield of $[\text{RuCo}(\text{CO})_6(\mu_2:\eta^1\text{-SCH}_2\text{CH}_2\text{AsMe}(\text{C}_6\text{H}_4\text{CH}_2\text{OMe}))]$ (**5**) was obtained. This was characterised by the use of standard spectroscopic techniques. The complex gave a molecular ion in the FAB mass spectrum consistent with the sequential loss of carbonyl ligands. The presence of stereogenic As and S centres, with even framework chirality gave a complex ^1H NMR spectrum, albeit without the complication of coupling to the donor atom, which was assigned on chemical shift data. The methylene protons of the arsinoethanethiol ligand gave a series of unresolved multiplets between 1.6 and 2.50 ppm each integrating for one proton. The signal at 1.38 ppm was assigned to the AsMe group, while the signal at 4.08 ppm was assigned to the benzylic protons giving the expected AB pattern. The down-field singlet at 3.04 ppm was assigned to the methoxy protons. The ^{13}C NMR spectrum was similarly informative, assigned with the aid of DEPT experiments, with the signals at 13.2 and 58.0 ppm assigned to the AsMe and OMe moieties, respectively. The signals assigned to the phenyl carbons were partly obscured by solvent peaks but those of the metal-bound carbonyls are assigned to the four separate signals in the usual region, ca. 190–210 ppm.

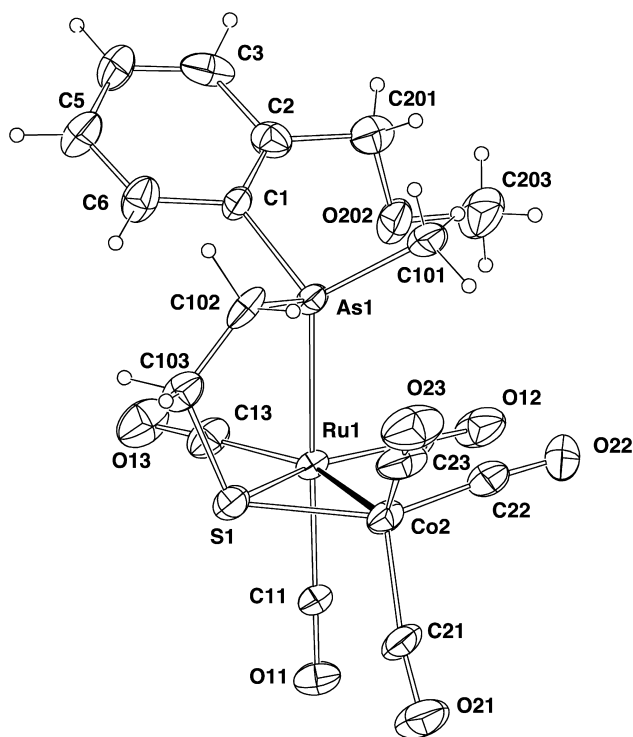


Fig. 4. Molecular projection of the structure of **5**.

Compound **5** crystallizes unsolvated with one neutral molecule, devoid of crystallographic symmetry, in the asymmetric unit. The determination, somewhat imprecise, by virtue of twinning problems, confirms the stoichiometry, connectivity and stereochemistry as given above and in Fig. 4 and Table 4. A search of the Cambridge Structural Database [30] found no structurally characterised Ru–Co dimers of this type. However one complex has some relevant elements that can be considered, $[(\mu_3\text{-S})\text{RuCo}_2(\text{CO})_8(\text{PMe}_2\text{Ph})]$ [31]. This complex is trimetallic with a μ_3 -sulfide ligand, not strictly comparable to **5**. The two Ru–Co bonds in $[(\mu_3\text{-S})\text{RuCo}_2(\text{CO})_8(\text{PMe}_2\text{Ph})]$ (2.666 Å (< >)) are not non-trivially different to the Ru–Co bond (2.689(2) Å) in **5**. While the Ru–S bond in **5** of 2.354(2) is only marginally different from that found in the trimetallic complex, 2.364(2), with similar in significant differences are seen in the Co–S distance: 2.203(3) in **5** and 2.173(3); 2.202(3) Å in $[(\mu_3\text{-S})\text{RuCo}_2(\text{CO})_8(\text{PMe}_2\text{Ph})]$.

The reaction of $[\text{Ru}_3(\mu\text{-dppm})(\text{CO})_{10}]$ with the secondary phosphine $\text{HPMe}(\text{C}_6\text{H}_4\text{CH}_2\text{OMe})$ gave, on one occasion, the trinuclear cluster $[\text{Ru}_3(\text{CO})_5(\text{dppm})(\text{PMe}(\text{C}_6\text{H}_4\text{CH}_2\text{OMe}))_4]$ (**6**), and on another occasion the oxide cluster $[\text{Ru}_3\text{H}(\text{CO})_7(\text{dppm})(\mu_2, \eta^1\text{-P(=O)Me}(\text{C}_6\text{H}_4\text{CH}_2\text{OMe}))]$ (**7**). It appears that the highly air-sensitive phosphine had a appreciable amount of the P(V) oxide present, as evident from the number of impurities detected by ^{31}P NMR of the remaining ligand. This serendipitous event has allowed us to examine the effect of coordination of the phosphine oxides to metals. The complexes proved too insoluble to obtain meaningful NMR data although giving adequate microanalyses.

Compound **6** crystallizes with one neutral molecule, devoid of crystallographic symmetry in the asymmetric unit of the structure, together with residues modelling as a dichloromethane disolvate; the latter are rife with disorder, also found throughout the phenyl ring 51 and more widely among diverse methoxyl pendants, although site occupancies, 0.5 throughout these latter, seemingly differ from those of the solvent components (ca. 1/3) and may not be concerted. The molecular core is well-defined, conforming the stoichiometry, connectivity and stereochemistry proposed above (see Table 5, Fig. 5). The molecule comprises an open Ru_3 triangle, $\text{Ru}(1)\cdots\text{Ru}(2)$ 3.8890(5) Å, $\text{Ru}(1,2)$ bridged by the P-dppm- P' ligand, seemingly

Table 4
Selected geometries (**5**)

Atoms	Parameter	Atoms	Parameter
<i>Distances</i> (Å)			
Ru(1)–Co(2)	2.689(2)	Co(2)–S(1)	2.203(3)
Ru(1)–S(1)	2.354(2)	Ru(1)–As(1)	2.461(1)
<i>Angles</i> (°)			
Ru(1)–Co(2)–S(1)	56.48(7)	Co(2)–Ru(1)–S(1)	51.27(7)
Co(2)–S(1)–Ru(1)	72.25(8)	Co(2)–Ru(1)–As(1)	87.98(5)
Ru(1)–S(1)–C(103)	106.7(3)	S(1)–Ru(1)–As(1)	86.03(7)
Co(2)–S(1)–C(103)	112.6(3)		

Table 5
Selected geometries (6)

Atoms	Parameter	Atoms	Parameter
<i>Distances</i> (Å)			
Ru(1)–Ru(3)	2.9394(5)	Ru(2)–Ru(3)	2.9716(5)
Ru(1)–P(1)	2.3892(7)	Ru(2)–P(2)	2.3961(7)
Ru(1)–P(5)	2.3473(8)	Ru(2)–P(3)	2.3632(7)
Ru(1)–P(6)	2.3758(7)	Ru(2)–P(4)	2.4049(7)
Ru(1)–C(11)	1.921(3)	Ru(2)–C(21)	1.916(3)
Ru(1)–C(12)	1.851(3)	Ru(2)–C(22)	1.855(3)
Ru(3)–P(6)	2.3700(8)	Ru(3)–P(4)	2.3625(7)
Ru(3)–P(5)	2.3376(8)	Ru(3)–P(3)	2.3334(8)
Ru(3)–C(31)	1.834(3)	Ru(1)··Ru(2)	3.8890(5)
<i>Angles</i> (°)			
Ru(1)–Ru(3)–Ru(2)	82.28(1)	P(1)–C(0)–P(2)	121.7(2)
C(0)–P(1)–Ru(1)	124.9(2)	C(0)–P(2)–Ru(2)	119.57(8)
P(1)–Ru(1)–Ru(3)	117.70(2)	P(2)–Ru(2)–Ru(3)	116.04(3)
P(1)–Ru(1)–P(6)	96.88(3)	P(2)–Ru(2)–P(4)	99.61(2)
P(1)–Ru(1)–P(5)	168.29(3)	P(2)–Ru(2)–P(3)	163.57(7)
P(1)–Ru(1)–C(12)	93.05(9)	P(2)–Ru(2)–C(22)	94.43(8)
Ru(1)–P(6)–Ru(3)	76.54(2)	Ru(2)–P(4)–Ru(3)	77.11(2)
Ru(1)–P(5)–Ru(3)	77.72(2)	Ru(2)–P(3)–Ru(3)	78.50(2)
P(5)–Ru(1)–P(6)	78.15(3)	P(4)–Ru(2)–P(3)	78.50(3)
P(5)–Ru(3)–P(6)	78.51(3)	P(4)–Ru(3)–P(3)	79.96(3)

Deviations of P(*n*) from the Ru₃ plane are (*n* = 1–6): 1.321(2), 1.812(2), –1.688(1), 1.244(1), –1.227(1), 1.694(1) Å.

under some strain, since P–C–P is very large (121.7(3)°, and Ru(3). The pairs of bonded ruthenium atoms are bridged by pairs of PMeAr (Ar=MeOCH₂C₆H₄) ligands; all ruthenium atoms have their coordination spheres completed by equatorial carbonyl groups, together with further axial groups in the case of Ru(1,2); the molecular

[(dppm){Ru(CO)₂(μ-P)₂]₂Ru core has putative *m* symmetry, broken at the molecular periphery by the dispositions of the phosphorus substituents, most notably by the differing methyl dispositions at P(3,5), that at P(3), being ‘axial’, while that at P(5) is ‘equatorial’, perhaps a consequence of the general crowding at the Ru(3) end of the molecule. All phosphorus atoms, except P(3,5) lie well above the Ru₃ plane. Axial and equatorial Ru–C (carbonyl) distances about Ru(1,2) differ systematically and significantly.

The overall structure adopted by [Ru₃(CO)₅(dppm)(μ₂-PMe(C₆H₄CH₂OMe))₄] (6), appears to be unique with no examples of a trinuclear, open-triangular cluster that contains six phosphine/phosphide donors found in the CSD [30]. The individual phosphides bridge the metal–metal bonds, a motif that is well known in the literature [32–40]. Much more common is a motif in which a triruthenium cluster has each Ru–Ru vector symmetrically bridged by phosphides, as exemplified by [Ru₃(CO)₉(μ-H)(μ-P(C₆H₁₁)₂)₃] [38].

Compound 7 crystallizes with one neutral molecule, devoid of crystallographic symmetry, comprising the asymmetric unit of the structure together with an accompanying CH₂Cl₂ hemi-solvate molecule which lies disordered about a crystallographic inversion centre, consistent with the stoichiometry, connectivity and stereochemistry as given above (Table 6, Fig. 6). The molecular core is the familiar (μ-H)Ru₃ array, chelated by *P*-dppm-*P'* with the bridging core hydride lying within the dppm chelate; the phosphine oxide is coordinated with the oxygen spanning the hydrido/dppm bridged ruthenium atoms, to the opposite site of the Ru₃ plane to the hydride (δH, 0.92(3); δO(3) ca. –1.709(1) Å)

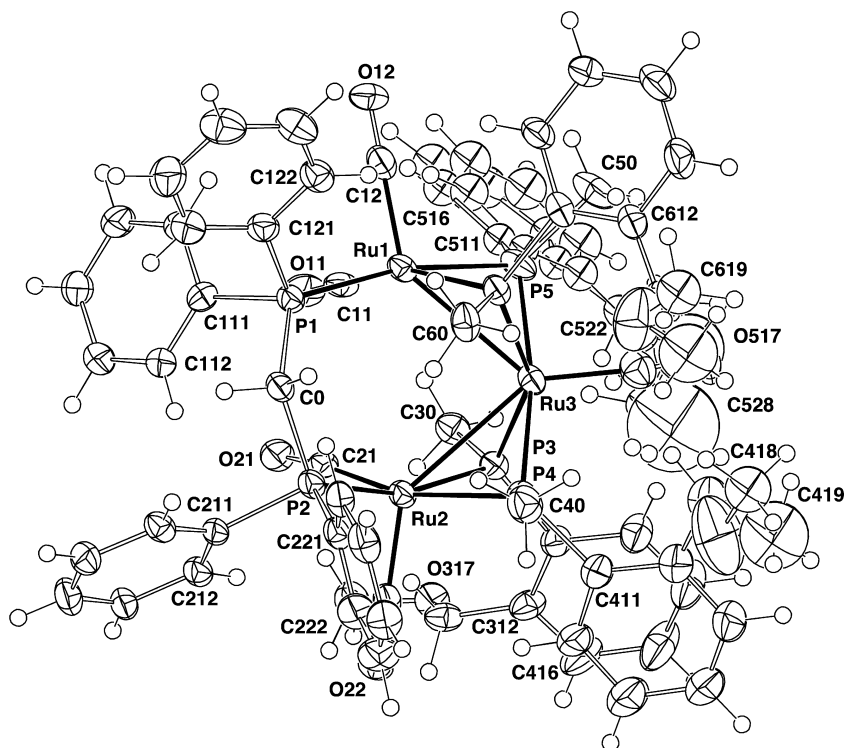


Table 6
 Selected geometries (7)

Atoms	Parameter	Atoms	Parameter
<i>Distances (Å)</i>			
Ru(1)–Ru(2)	2.7623(2)	Ru(1)–H(0)	1.67(3)
Ru(1)–Ru(3)	2.7656(2)	Ru(2)–H(0)	1.79(3)
Ru(2)–Ru(3)	2.7842(2)	Ru(2)–O(3)	2.198(1)
Ru(1)–O(3)	2.202(1)	Ru(2)–P(2)	2.3742(4)
Ru(1)–P(1)	2.3736(4)	Ru(2)–C(21)	1.849(2)
Ru(1)–C(11)	1.843(2)	Ru(2)–C(22)	1.891(2)
Ru(1)–C(12)	1.900(2)	Ru(3)–C(32)	1.909(2)
Ru(3)–C(31)	1.922(2)	Ru(3)–C(33)	1.915(2)
Ru(3)–P(3)	2.3311(5)		
<i>Angles (°)</i>			
Ru(2)–Ru(1)–Ru(3)	60.486(5)	Ru(1)–Ru(2)–Ru(3)	59.817(5)
Ru(2)–Ru(3)–Ru(1)	59.70(1)	P(1)–C(0)–P(2)	114.98(8)
Ru(1)–P(1)–C(0)	108.32(5)	Ru(2)–P(2)–C(0)	107.16(5)
P(1)–Ru(1)–Ru(2)	95.03(1)	P(2)–Ru(2)–Ru(1)	93.31(1)
P(1)–Ru(1)–Ru(3)	153.77(1)	P(2)–Ru(2)–Ru(3)	152.99(1)
P(1)–Ru(1)–O(3)	82.76(3)	P(2)–Ru(2)–O(3)	87.07(3)
Ru(1)–O(3)–Ru(2)	77.79(4)	O(3)–P(3)–Ru(3)	99.12(5)
Ru(1)–O(3)–P(3)	99.12(6)	Ru(2)–O(3)–P(3)	98.68(6)
Ru(1)–H(0)–Ru(2)	106(1)		

(the phosphorus atoms are also well out of plane, all to the same side as O(3): $\delta P(1,2,3)$ 0.416(2), 0.120(2) 2.127(1) Å). The $\{(PP)HRu_3(CO)_7PO\}$ molecular core has quasi-m symmetry, broken by the unsymmetrical substitution at P(3), and, peripherally, by the diverse phenyl orientations, most impressively in the (dppm)-P–Ru–O angles which differ by more than 4°. The Ru–C (carbonyl) (axial/equato-

rial) distances at Ru₃ are closely ranged ($< 0.1_3$ Å); the differences in the Ru–C (carbonyl) distances at Ru(1,2) are substantial, Ru-(quasi-)equatorial being longer than their (less crowded) axial counterparts by ca. 0.04₅ Å. Ru–C–O are all greater than 176.9°, excepting Ru(1)–C(12)–O(12) which is reduced to 172.6(2)°, perhaps in consequence of the proximity of the phenyl substituent, but it is notable that contacts are more obvious to other carbonyls. Table 7 summarizes the crystallographic/refinement data for all the compounds studied.

Phosphine oxides do not generally make good ligands but are known to undergo reactions with oxophilic metals [41]. There are few structurally characterised examples of such complexes in the literature although the reaction of $[Ru_3(CO)_{12}]$ with $Ph_2P(O)CCBu^t$ has given the binuclear example $[Ru_2(CO)_6(\mu_2:\eta^2-CCBu^t)(\mu-Ph_2P=O)]$ [42]. The only example of coordination of a PO moiety in a similar manner to that observed in 7 is found in $[Ru_3(CO)_9(\mu-P(OMe)_3)]$ [43]. In this case the P(III) ligand has utilised the oxygen lone pairs to participate in bonding and is presumably a thermolysis product of $[Ru_3(CO)_{11}(P(OMe)_3)]$ which was also isolated in the reaction of $[Ru_3(CO)_{12}]$ with $(MeO)_2PN(Me)N(Me)P(OMe)_2$. However, it is unclear whether 7 is the product of the reaction of 1 with the P(V), compound $HP(O)Me(C_6H_4CH_2OMe)$ or the oxidation of a pre-formed cluster containing a phosphide ligand. What is known is that μ_3-P ligands can be oxidised, with the PO thus formed retained in the structure [41] but it is also known that 1 tends to add more than one secondary

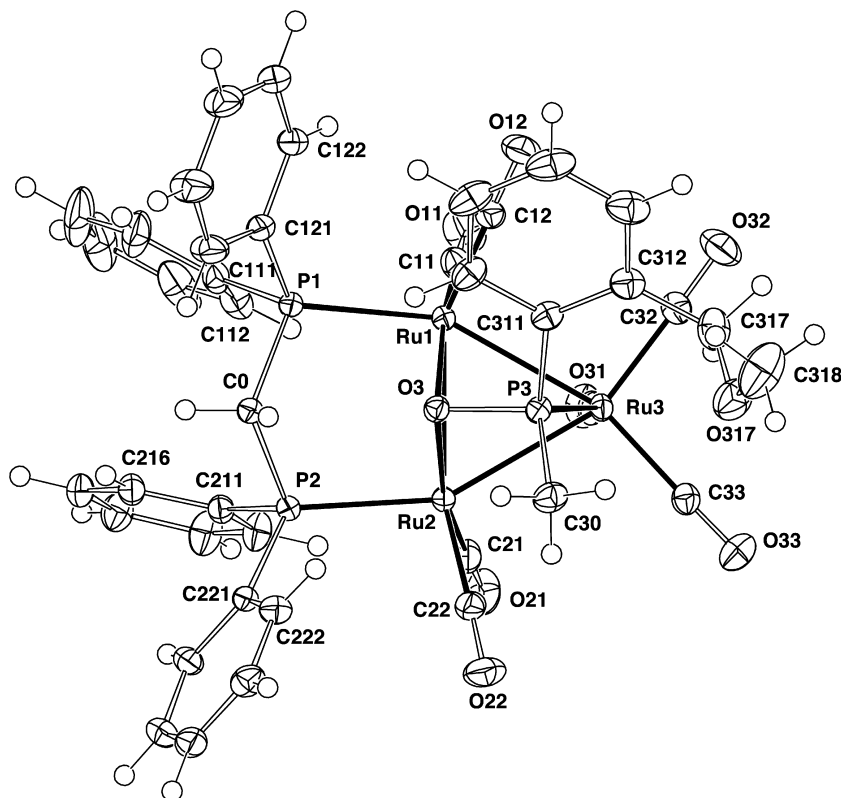


Fig. 6. Molecular projection of the structure of 7.

Table 7
Crystal/refinement data

Compounds	2	3 · C ₂ H ₆ O	4	5	6 · 2CH ₂ Cl ₂	7 · 1/2CH ₂ Cl ₂
Formula	C ₄₀ H ₃₃ O ₇ P ₃ Ru ₃ S	C ₇₈ H ₆₁ O ₁₈ P ₅ Ru ₆ S	C ₂₆ H ₁₈ O ₁₀ P ₂ Ru ₄ S ₂	C ₁₇ H ₁₆ AsCoO ₇ RuS	C ₆₈ H ₇₄ Cl ₄ O ₉ P ₆ Ru ₃	C _{41.5} H ₃₆ ClO ₉ P ₃ Ru ₃
<i>M_r</i> (Dalton)	1053.9	2079.7	1020.8	599.3	1666.2	1110.3
Crystal system	Monoclinic	Triclinic	Triclinic	Monoclinic	Triclinic	Triclinic
Space group	<i>P</i> 2 ₁ / <i>c</i> (No. 14)	<i>P</i> $\bar{1}$ (No. 2)	<i>P</i> $\bar{1}$ (No. 2)	<i>P</i> 2 ₁ / <i>c</i> (No. 14)	<i>P</i> $\bar{1}$ (No. 2)	<i>P</i> $\bar{1}$ (No. 2)
<i>a</i> (Å)	15.579(1)	18.330(2)	8.9638(8)	9.077(8)	12.930(2)	9.6316(7)
<i>b</i> (Å)	12.6060(9)	21.979(3)	18.468(2)	11.431(6)	15.620(2)	12.2357(9)
<i>c</i> (Å)	20.685(2)	23.603(3)	20.384(2)	20.470(6)	19.432(3)	19.032(1)
α (°)		106.888(2)	72.423(3)		82.840(2)	83.686(3)
β (°)	103.405(2)	112.276(2)	83.966(4)	91.38(5)	80.687(2)	78.008(2)
γ (°)		98.504(2)	83.479(4)		88.633(2)	75.498(2)
<i>V</i> (Å ³)	3952	8054	3187	2123	3843	2120
<i>D</i> _{calc} (g cm ⁻³) (<i>Z</i>)	1.77 ₁ (4)	1.71 ₅ (4)	2.12 ₇ (4)	1.87 ₄ (4)	1.44 ₀ (2)	1.73 ₉ (2)
μ _{Mo} (mm ⁻¹)	1.36	1.29	1.13	3.2	0.90	1.29
Specimen (mm)	0.45, 0.35, 0.25	0.35, 0.21, 0.06	0.06, 0.03, 0.015	0.60, 0.45, 0.30	0.32, 0.28, 0.22	0.50, 0.40, 0.33
<i>T</i> _{min/max}	0.84	0.87	(No corrections)	0.79	0.72	0.90
2 θ _{max} (°)	75	58	43	50	60	75
<i>N</i> _t	78 323	74 966	15 053	–	37 013	43 474
<i>N</i> (<i>R</i> _{int})	20 600 (0.040)	39 094 (0.039)	13 497	3738	13 300 (0.051)	21 692 (0.019)
<i>N</i> _o	15 991	25 823	11 738	2353	9983	18 368
<i>R</i> ₁	0.041	0.050	0.069	0.084	0.072	0.033
<i>wR</i> ₂	0.10	0.12	0.17	0.089	0.22	0.074

phosphine to give complexes such as [Ru₃(CO)₆(μ-H)₂(μ-PR₂)₂(μ-dppm)] [35] rather than [Ru₃(CO)₈(μ-H)(μ-PR₂)(μ-dppm)].

The PO distance in [Ru₃(CO)₉(μ-P(OMe)₃)] [43] 1.64(1) Å (<>, two independent molecules) is only marginally different to that of **7**, 1.615(1) Å and suggestive of a single PO bond. Similarly the Ru–P(O) distances are also directly comparable to those of **7**. It is of interest is that in neither case of complexes **6** or **7**, did the benzyl methoxy substituent become involved in the bonding, presumably a consequence of steric constraints.

4. Conclusions

We have found that several pnictogen based multifunctional ligands interact with either [Ru₃(CO)₁₀(μ-dppm)] or [Ru₃(CO)₁₂] to form a number of unusual new complexes, in which the phenylphosphinoethanethiol ligand LH₂ may upon deprotonation bind intramolecularly or span two [Ru₃(CO)_{*x*}(μ-dppm)] moieties. The retention of the PH functionality in both **2** and **3** suggests that the thiol unit is much more reactive in these cases giving both a bridging hydride and a bridging sulfide. While not strictly comparable, HSCH₂CH₂AsMe(C₆H₄CH₂OMe), in its reaction with [RuCo₂(CO)₁₁] also produced similar results as well as cluster breakdown as seen in the structure of **5**. However, more forcing conditions could implicate the PH group in a reaction with μ₂-S and μ₂-P groups found in the structure of complex **4**. The reactivity of a secondary phosphine was clearly illustrated in the reaction of HPMe(C₆H₄CH₂OMe) with **1**, which in the case of complex **6**, gave a product with an unprecedented structure, and, with **7**, showed that oxidation is possible, although it is not clear at what point this has occurred.

Although, the multiple stereogenic centres present in the ligands and complexes rendered their spectroscopic characterisation difficult, their influence was clearly observed. Once again it has been shown that metal–metal bonding does not impart any higher degree of structural integrity and that a complex interplay of electronic and steric effects is evident in these complexes.

Acknowledgements

We thank the Australian Research Council for funding part of this work. NSH was the holder of an Australian Postgraduate Award. Use of the ChemMatCARS Sector 15 at the Advanced Photon Source, was supported by the Australian Synchrotron Research Program, which is funded by the Commonwealth of Australia under the Major National Research Facilities Program. ChemMatCARS Sector 15 is also supported by the National Science Foundation/Department of Energy under Grant numbers CHE9522232 and CHE0087817 and by the Illinois Board of Higher Education. The Advanced Photon Source is supported by the U.S. Department of Energy, Basic Energy Sciences, Office of Science, under Contract No. W-31-109-Eng-38.

Appendix A. Supplementary material

CCDC 664866, 664867, 664868, 664869, 664870, 664871 contain the supplementary crystallographic data for this paper. These data can be obtained free of charge from The Cambridge Crystallographic Data Centre via www.ccdc.cam.ac.uk/data_request/cif. Supplementary data associated with this article can be found, in the online version, at [doi:10.1016/j.jorganchem.2008.01.040](https://doi.org/10.1016/j.jorganchem.2008.01.040).

References

- [1] A.J. Bailey, S. Basra, P.J. Dyson, *Green Chem.* (1999) 31–32.
- [2] S. Rossini, *Catal. Today* 77 (2003) 467–484.
- [3] R.J. Angelici, *Acc. Chem. Res.* 21 (1988) 387–394.
- [4] C.M. Friend, J.T. Roberts, *Acc. Chem. Res.* 21 (1988) 394.
- [5] W.-T. Wong, K.S.-Y. Leung, *J. Chem. Soc., Dalton Trans.* (1999) 2077–2086.
- [6] R.C. Brady III, R. Pettit, *J. Am. Chem. Soc.* 102 (1980) 6181.
- [7] E.L. Muetterties, *Science* 196 (1977) 839.
- [8] T. Tanase, R.A. Begum, H. Toda, Y. Yamamoto, *Organometallics* 20 (2001) 968.
- [9] F. Zaera, *Chem. Rev.* 95 (1995) 2651.
- [10] P. Braunstein, J. Rose, in: P. Braunstein, L.A. Oro, P.R. Raithby (Eds.), *Metal Clusters in Chemistry Metal Clusters in Chemistry*, vol. 2, Wiley-VCH, Weinheim, 1999, pp. 616–677.
- [11] R.J. Angelici, *NATO ASI Series, Series 3: High Technology* 60 (1998) 89–127.
- [12] P. Braunstein, J. Rose, in: R.D. Adams, F.A. Cotton (Eds.), *Catalysis by Di- and Polynuclear Metal Cluster Complexes*, Wiley-VCH, New York, 1998, pp. 443–508.
- [13] D.F. Shriver, H.D. Kaesz, R.D. Adams, *The Chemistry of Metal Cluster Complexes*, VCH, New York, 1990.
- [14] A.W. Coleman, D.F. Jones, P.H. Dixneuf, C. Brisson, J.-J. Bonnet, G. Lavigne, *Inorg. Chem.* 23 (1984) 952–956.
- [15] A.A. Torabi, A.S. Humphreys, G.A. Koutsantonis, B.W. Skelton, A.H. White, *J. Organomet. Chem.* 655 (2002) 227–232.
- [16] M.I. Bruce, G.A. Koutsantonis, M.J. Liddell, B.K. Nicholson, *J. Organomet. Chem.* 320 (1987) 217–227.
- [17] N. Lugan, J.-J. Bonnet, J.A. Ibers, *Organometallics* 7 (1988) 1538–1545.
- [18] N. Lugan, J.-J. Bonnet, J.A. Ibers, *J. Am. Chem. Soc.* 107 (1985) 4484–4491.
- [19] M.I. Bruce, P.A. Humphrey, B.W. Skelton, A.H. White, M.L. Williams, *Aust. J. Chem.* 38 (1985) 1301.
- [20] M.I. Bruce, B.K. Nicholson, M.L. Williams, *Inorg. Synth.* 26 (1990) 225.
- [21] S. Chaudhury, S. Blaurock, E. Hey-Hawkins, *Eur. J. Inorg. Chem.* (2001) 2587–2596.
- [22] G.M. Sheldrick, *SHELXL-97: A Program for Crystal Structure Refinement*, University of Göttingen, 1997.
- [23] P. Fompeyrine, G. Lavigne, J.-J. Bonnet, *J. Chem. Soc., Dalton Trans.* (1987) 91–95.
- [24] J.A. Cabeza, I. del Rio, L. Martinez-Mendez, D. Miguel, *J. Organomet. Chem.* 692 (2007) 4407–4410.
- [25] G. Hogarth, N. Hadj-Bagheri, N.J. Taylor, A.J. Carty, *J. Chem. Soc., Chem. Commun.* (1990) 1352–1353.
- [26] H. Vahrenkamp, *J. Organomet. Chem.* 370 (1989) 65–73.
- [27] H. Vahrenkamp, *Comments Inorg. Chem.* 4 (1985) 253–267.
- [28] H. Vahrenkamp, *Adv. Organomet. Chem.* 22 (1983) 169–208.
- [29] H. Vahrenkamp, *Phil. Trans. Roy. Soc. London, Ser. A* 308 (1982) 17–26.
- [30] F.H. Allen, *Acta Crystallogr. B* 58 (2002) 380–388.
- [31] H. Bantel, W. Bernhardt, A.K. Powell, H. Vahrenkamp, *Chem. Ber.* 121 (1988) 1247–1256.
- [32] A.D. Phillips, A. Ienco, J. Reinhold, H.-C. Bottcher, C. Mealli, *Chem. Eur. J.* 12 (2006) 4691–4701.
- [33] H.-C. Boettcher, D. Himmel, M. Scheer, *Organometallics* 23 (2004) 5314–5316.
- [34] H.-C. Bottcher, M. Fernandez, M. Graf, K. Merzweiler, C. Wagner, *Z. Anorg. Allg. Chem.* 628 (2002) 2247–2248.
- [35] H.-C. Bottcher, M. Graf, C. Wagner, *Phosphorus, Sulfur and Silicon and the Related Elements* 168–169 (2001) 509–512.
- [36] H.C. Bottcher, M. Graf, K. Merzweiler, T. Rosel, H. Schmidt, C. Wagner, *Polyhedron* 20 (2001) 2011–2018.
- [37] H.C. Bottcher, M. Graf, K. Merzweiler, C. Wagner, *J. Organomet. Chem.* 628 (2001) 144–150.
- [38] H.-C. Bottcher, M. Graf, K. Merzweiler, C. Bruhn, *Polyhedron* 17 (1998) 3433–3438.
- [39] M. Graf, K. Merzweiler, C. Bruhn, H.-C. Bottcher, *J. Organomet. Chem.* 553 (1998) 371–378.
- [40] H.-C. Bottcher, M. Graf, K. Merzweiler, C. Bruhn, *Polyhedron* 16 (1997) 3253–3260.
- [41] B.T. Sterenberg, L. Scoles, A.J. Carty, *Coord. Chem. Rev.* 231 (2002) 183–197.
- [42] D.E. Fogg, N.J. Taylor, A. Meyer, A.J. Carty, *Organometallics* 6 (1987) 2252–2254.
- [43] S.G. Bott, J.C. Wang, M.G. Richmond, *J. Chem. Crystallogr.* 29 (1999) 587–595.